Exploring magnetic plasmon polaritons in optical transmission through hole arrays perforated in trilayer structures

Tao Li,[a),b)] Jia-Qi Li, Fu-Ming Wang, Qian-Jin Wang, Hui Liu, Shi-Ning Zhu,[a),c)] and Yong-Yuan Zhu
National Laboratory of Solid State Microstructures, Nanjing University, Nanjing 210093, China

(Received 19 March 2007; accepted 26 May 2007; published online 21 June 2007)

Optical transmission properties through hole arrays in metal/dielectric/metal trilayer structures were demonstrated. Besides the surface plasmon induced strong transmission and well-recognized negative refraction band, a higher mode was observed and elaborately investigated. Detailed results showed that this mode belongs to a higher magnetic excitation related to the reciprocal vector $G_{1,1}$ of the lattice, and a "magnetic plasmon polariton (MPP)" model was proposed to describe such magnetic excitations in periodically modulated structure. By adjusting the structural parameters, the authors can conveniently control the MPPs' properties, which provide us another way to tailor the light propagation properties in subwavelength structures. © *2007 American Institute of Physics*. [DOI: 10.1063/1.2750394]

The desire to manipulate the photon's behavior in a controlled manner in micro-nanoscale has inspired good many researches and leads to a new discipline—plasmonics owing to its ability to merge electronics and photonics.[1,2] Surface plasmon polaritons (SPPs) stemmed from the coupling of electromagnetic wave and the collective electronic excitations on metal surface especially attracted many interests considerably due to its important role in the extraordinary optical transmission (EOT) phenomena since Ebbesen's report in 1998.[3–5] Although SPP excitation is recognized as not the only mechanism responsible for EOTs in recent studies,[6–8] its remarkable contribution in the interaction between the light and metallic nanostructures is undoubted. At the same time, in another very active topic of negative index metamaterial (NIM), great efforts have been made to seek smart structures to have high coupling to the magnetic-field component of light, which produces a negative permeability to meet the negative refractive (NR) property.[9,10] In a common sense, one would imagine could a plasmonic behavior be formed via the coupling to the magnetic component of incident wave in a proper metamaterial? Here, we reintroduce the metal/dielectric/metal trilayer structure perforated with square-hole arrays [or so-called "fishnet" structure, sketched in Fig. 1(a)], which was well developed in recent NIM studies.[11–13]

The proposed structure was proved to exhibit magnetic response via two coupled metal layers referred as "magnetic atoms." In the top view [Fig. 1(b)], the horizontal blocks filled with red diagonal patterns (type M1) are the commonly identified magnetic atoms, and the longitudinal stripes are regarded as the electric atoms to produce the negative permittivity.[11,12] However, from another point view, magnetic resonance may not be always localized but coupled to its neighborhoods by magnetic inductions.[14–16] So in our considerations, when magnetic resonances are excited in the region M1, they will most possibly spread away into those "electric atoms." Thus, more magnetic atoms would be formed inside the middle layer of the longitudinal strips, which are sketched as types M2 and M3 (it is only a schematic, more types may exist for higher modes). Thus, a plasmonic behavior comes into being in a magnetic induction way. Different plasmon modes will be excited as is coupled to appropriate incident light. So we call such magnetic excitations as "magnetic plasmon polaritons" (MPPs).

To verify this idea, trilayer ($Ag/SiO_2/Ag$) samples with square-hole arrays are fabricated on polished K9-glass substrates. Experimentally, the trilayer films are prepared by sputtering, and then followed with the milling of focused-ion beam (Strata FIB 201, FEI Company, 30 keV Ga ions). By controlling the sputtering condition and focused-ion beam (FIB)-milling treatment, the sample structural parameters can be adjusted conveniently. Here, two series of samples are addressed, both of whose Ag film thickness (t=35 nm) and hole size (a=250 nm) are kept unchanged, but various SiO_2

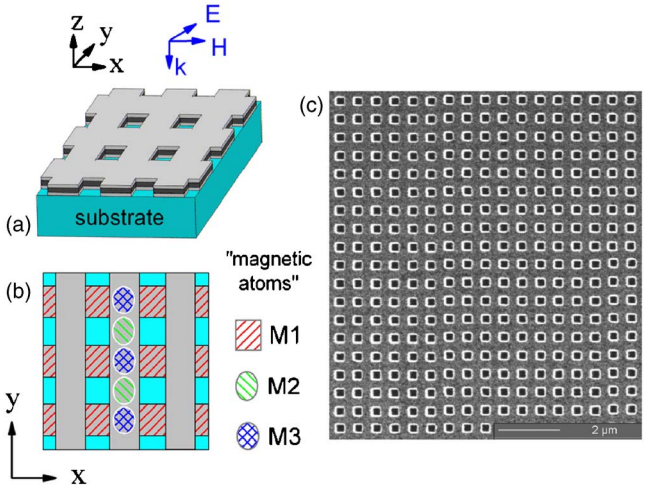

FIG. 1. (Color online) (a) Schematic of the $Ag/SiO_2/Ag$ trilayer structure perforated with square-hole array on a K9-glass substrate. (b) Top view of the structure, where longitudinal strips are commonly considered "electric atoms" and horizontal blocks marked as M1 are the "magnetic atoms." M2 and M3 are the proposed magnetic atoms excited inside the strips. (c) Top view of a typical FIB image of the fabricated sample A with a scale bar of 2 μm.

[a)]Authors to whom correspondence should be addressed.
[b)]Electronic mail: litaonju@eyou.com
[c)]Electronic mail: zhunsn@nju.edu.cn

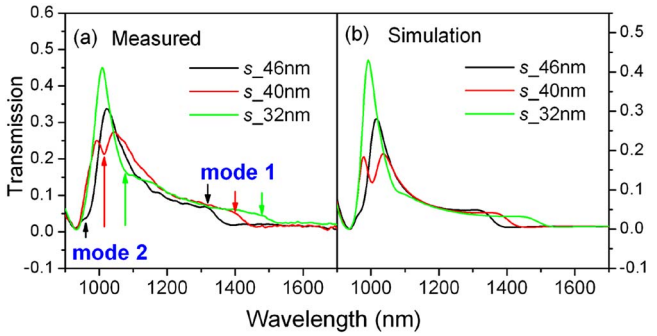

FIG. 2. (Color online) Experimentally measured (a) and numerical calculated (b) transmission spectra of the samples A, B, and C with various SiO_2 spacers, in which mode 1 and mode 2 are marked out as two MPP modes.

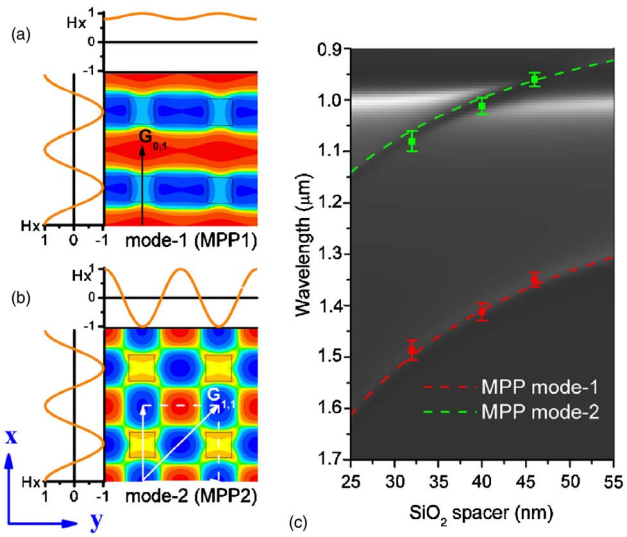

FIG. 3. (Color online) Simulated magnetic field H_x distribution maps for mode 1 (a) and for mode 2 (b), in the xy plane (z=0) in the center of the middle SiO2 layer. Normalized intensities of H_x in the map borders and associated reciprocal vectors for two cases are marked out in the maps. (c) Calculated transmittance map of 30 samples as s range from 25 to 55 nm, in which the symbols with error bars are the experimental data and the dashed lines are the fitting curves according to Eq. (3). The strong transmission about 1000 nm is the SPP mode.

spacer thicknessess (s) with fixed lateral period (P_x=P_y =600 nm) for samples A/B/C, and various periods in the x axis (P_x) with fixed SiO_2 spacer (s=46 nm).for samples A1/A2/A3. Each sample possesses an array containing 81×81 =6561 holes, and covers an area about 49×49 μm^2 (more for samples A1/A2/A3 for their enlarged P_x). Figure 1(c) shows a typical FIB image of sample A, revealing a well arranged square-hole array.

In investigations, the tabulated samples are planted on a home-built optical setting with an illumination of a 50 W halogen lamp. A polarized light (y polarization) is incident normal to the sample plane after a slight focalization, and the nearly zero-order transmissions are collected by an optical-spectrum analyzer (ANDO AQ-6315A) via a fiber coupler. Figure 2(a) shows the three measured transmission spectra of the samples A/B/C with corresponding s of 46/40/32 nm. Besides the major transmission peak located around 1000 nm, which is due to the SPP mode of $G_{1,0}$ on Ag/SiO_2 interface,[17] two remarkable features are observed. First, there is a clear transmission step at longer wavelength region manifesting a very similar appearance to the original work,[11] which is the well-known magnetic response leading to the NR property. By changing s, the eigenfrequency alternates along the formula $\omega=(L_{\text{eff}}C_{\text{eff}})^{1/2}$, where L_{eff} and C_{eff} are the effective inductance and capacitance of equivalent LC circuit composed by two metal layers. Merely from this point, this magnetic response only seems to be a common magnetic resonance. However, the second characteristic of the spectra brings us an important clue that there is another mode closely related to first mode, which appears more like a dip inside the strong SPP transmissions. In fact, this high "dip" mode was observed in previous reports,[12,13] but no discussion was addressed. By careful inspection on our results, we find that the ratio of the frequency of this higher mode (mode 2) over the first mode (mode 1) is nearly 1.4 for all these samples. It suggests that the eigenfrequency of mode 2 is about $\sqrt{2}$ times the mode 1, very like a (1,1) mode of the magnetic plasmon excitation.

The subsequent numerical simulations confirm this assumption. High frequency structure simulator (HFSS), a commercial software package based on the finite elemental method, is employed in simulations. The dielectric constant of silver is defined by the Drude model $[\varepsilon=1-\omega_p^2/(\omega^2+i\omega\gamma)]$, with the plasma frequency $\omega_p=1.38\times10^{16}$ s^{-1} and collision frequency $\gamma=8.5\times10^{13}$ s^{-1}.[13] The refractive indices of SiO_2 spacer and glass substrate are set as 1.47 and 1.5, respectively, according to the material's data. From simulations, the transmission spectra are well reproduced, as shown in Fig. 2(b), except for a little difference in intensities. The characteristic peaks or dips also demonstrate the ratio of $\lambda_{\text{mode 1}}/\lambda_{\text{mode 2}}$ approximately equals 1.4. To get a clear cognition, Figs. 3(a) and 3(b) reveal the simulated magnetic field (H_x) distributions in the xy plane (z=0) lying in the center of the SiO_2 spacer for those two modes. Wavelike features of magnetic field are well presented in the y direction for mode 1 and in both the x and y directions for mode 2. It confirms the plasmonic character of MPPs modulated by the lateral periodic structure. As well as the reciprocal vector $G_{0,1}$ associated mode 1 (MPP1), mode 2 (MPP2) is apparently related to $G_{1,1}$ [as illustrated in Fig. 3(b)]. For the normal incidence, we can presumably propose the MPP excitation condition in the form analogous to that of the SPPs on perforated metal surface as

$$\lambda_{\text{MPP}}=\frac{2\pi c}{|G_{m,n}|}\left(\frac{1}{\omega_{LC}}\right), \tag{1}$$

where

$$G_{m,n}=m\frac{2\pi}{P_x}\hat{x}+n\frac{2\pi}{P_y}\hat{y} \tag{2}$$

is the (m,n) ordered in-plane reciprocal vector of the hole lattice, and ω_{LC} is the eigenfrequency of the LC circuit induced magnetic resonance. It should be noted that, as the magnetic excitation is polarization dependent, the orthogonal modes cannot be excited for a polarized incidence. For example of y polarization, all $(m,0)$ modes are extinct. As for the concerned samples with a square lattice P_x=P_y, we have $|G_{1,0}|=|G_{0,1}|$ and $|G_{1,1}|=\sqrt{2}|G_{0,1}|$. It truly verifies the $\sqrt{2}$ relation of these two modes, indicating a feature very analogous to the SPPs. From the H_x maps, we also can identify the exact "moment" arrangements of the magnetic atoms M1, M2, and M3 schemed in Fig. 1(b) in correspondence to these two MPP modes.

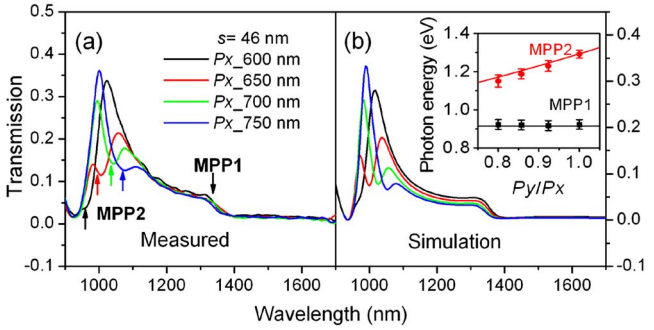

FIG. 4. (Color online) Measured (a) and calculated (b) transmission spectra of samples A/A1/A2/A3 with various P_x. Inset of (b) is the calculated eigen frequency of MPPs according to Eq. (4) (lines) and the experimental data (symbols) as functions of P_y/P_x.

Furthermore, Fig. 3(c) gives an overview transmittance of the calculated 30 samples with s ranging from 25 to 55 nm, which is depicted on an intuitive gray scale (black corresponds to zero and white to 0.6). The mode MPP1 as a transmission step and MPP2 as a dip are clearly exhibited; the dashed lines are the fitting curves following the formula

$$\lambda_{\mathrm{MPP1}} = \frac{2\pi c}{\omega_{LC}} \approx 2\pi c (L_{\mathrm{eff}} C_{\mathrm{eff}})^{-1/2}, \quad C_{\mathrm{eff}} = \varepsilon_s \frac{A}{s} + C_{\mathrm{ext}}, \tag{3a}$$

$$\lambda_{\mathrm{MPP2}} = \frac{|G_{0,1}|}{|G_{1,1}|} \lambda_{\mathrm{MPP1}} = \lambda_{\mathrm{MPP1}}/\sqrt{2}, \tag{3b}$$

where ε_s is the dielectric constant of SiO_2, A is the normalized capacitance area, and C_{ext} is an additional capacitance caused by edge and coupling effects. The symbols with error bars are the experimental data, which reveals an extremely good accordance with the theoretical results. Beyond these, another significant aspect from the map is the cutting feature of the strong SPP transmission band as the MPP2 mode crosses through, indicating a strong interaction between the two modes. It is likely to be a suppressed contribution of the MPP to the optical transmission, as is rightly located inside the wide SPP transmission band.

Followed with above discussions, we show the spectra of another series of samples (A/A1/A2/A3) in Fig. 4, in which the x period (P_x) of the array is changed from 600 to 750 nm with the fixed SiO_2 spacer (s=46 nm). Excellent agreement is also achieved between the measured results and the simulations. Both of them reveal the fact that the mode MPP2 redshifts obviously with increasing P_x, while the mode MPP1 kept unchanged. It is in good expectation that the MPP is modulated by the lattice parameters following

$$\frac{\omega_{\mathrm{MPP2}}}{\omega_{\mathrm{MPP1}}} = \frac{\lambda_{\mathrm{MPP1}}}{\lambda_{\mathrm{MPP2}}} = \frac{|G_{1,1}|}{|G_{0,1}|} = \left[1 + \left(\frac{P_y}{P_x}\right)^2\right]^{1/2}, \tag{4}$$

as ω_{MPP1} keeps constant due to the unchanged P_y. Inset of Fig. 4(b) demonstrates the calculated eigenfrequency of MPPs and the experimental data as the functions of P_y/P_x, which are in good agreement as well. Furthermore, as well demonstrated that strong EOT can be adjusted to a sharper peak or two split peaks, the SPP induced EOT property can be manipulated by the proposed MPPs in a controllable way.

From these results and interpretations, a clear physics picture is presented. When a light normally incidents into a perforated metal film, optical field is enhanced at proper wavelengths due to the excitation of the SPPs (or other surface waves). These em energies will reradiate through the holes array leading to a strong broad transmission band if only one metal layer is presented. However, the trilayer structure composes many magnetic resonators by LC circuits, which will absorb the em energies around their resonant frequency with relative narrow linewidth. If this mode is rightly located inside or near the transmission band, it will appear as a dip or a step in spectrum correspondingly. Notably, these magnetic responses are actually modulated by the periodic structure via the lateral coupling, thus multi-MPP modes are excited as different reciprocal vectors $G_{m,n}$ are involved, which behave in a similar manner of the $G_{m,n}$ associated SPP excitations.

In summary, by elaborately investigating the transmission property of perforated trilayer structure, we proposed a remarkable MPP model as a more basic cognition on the well-known magnetic response in this system. A higher magnetic mode that is emphatically illustrated as a MPP excitation associated the vector $G_{1,1}$ of the lattice, which revealed a suppression role to the SPP induced strong transmission. Along with this, the interaction between the MPP and SPP was discussed in detail. Moreover, other higher modes related to the lattice characters are believed to exist in similar structures, and these modes are considered providing another way to tailor the optical property of such metamaterials.

This work is supported by the National Natural Science Foundation of China (Grant Nos. 10534020, 10474042, 10604029, 10523001), the State Key Program for Basic Research of China under Grant No. 2006CB921804 and by the 111 project under Grant No. B07026, and by China Postdoctoral Science Foundation (No. 2006390928).

[1] S. A. Maier and H. A. Atwater, J. Appl. Phys. **98**, 1 (2005).
[2] E. Ozbay, Science **311**, 189 (2006).
[3] T. W. Ebbesen, H. J. Lezec, H. F. Ghaemi, T. Thio, and P. A. Wolff, Nature (London) **391**, 667 (1998).
[4] L. Martin-Moreno, F. J. Garcia-Vidal, H. J. Lezec, K. M. Pellerin, T. Thio, J. B. Pendry, and T. W. Ebbesen, Phys. Rev. Lett. **86**, 1114 (2001).
[5] W. L. Barnes, W. A. Murray, J. Dintinger, E. Devanx, and T. W. Ebbesen, Phys. Rev. Lett. **92**, 107401 (2004).
[6] H. J. Lezec and T. Thio, Opt. Express **12**, 3629 (2004).
[7] G. Gay, O. Alloschery, B. V. de Lesegno, and J. Weiner, and H. J. Lezec, Phys. Rev. Lett. **96**, 213901 (2006).
[8] P. Lalanne and J. P. Hugonin, Nat. Mater. **2**, 551 (2006).
[9] V. M. Shalaev, Nature Photonics **1**, 41 (2007).
[10] C. M. Soukoulis, S. Linden, and M. Wegener, Science **315**, 47 (2007).
[11] S. Zhang, W. Fan, N. C. Panoiu, K. J. Malloy, R. M. Osgood, and S. R. J. Brueck, Phys. Rev. Lett. **95**, 137404 (2005).
[12] G. Dolling, C. Enkrich, M. Wegener, C. M. Soukoulis, and S. Linden, Science **312**, 892 (2006)..
[13] G. Dolling, C. Enkrich, M. Wegener, C. M. Soukoulis, and S. Linden, Opt. Lett. **31**, 1800 (2006).
[14] E. Shamonina, V. A. Kalinin, K. H. Ringhofer, and L. Solymar, J. Appl. Phys. **92**, 6252 (2002).
[15] A. K. Sarychev, G. Shvets, and V. M. Shalaev, Phys. Rev. E **73**, 036609 (2006).
[16] H. Liu, D. A. Genov, D. M. Wu, Y. M. Liu, J. M. Steele, C. Sun, S. N. Zhu, and X. Zhang, Phys. Rev. Lett. **97**, 243902 (2006).
[17] Here, we do not want to be involved in the detailed discussions on the multicauses of the strong EOT, only regarded it as the SPP mode for simplifications.